

Structural, thermal and electrochemical cell characteristics of poly(vinyl chloride)-based polymer electrolytes

S. Ramesh^a, A.K. Arof^{b,*}

^a*Institute of Postgraduate Studies and Research, University Malaya, 50603 Kuala Lumpur, Malaysia*

^b*Physics Department, University Malaya, 50603 Kuala Lumpur, Malaysia*

Received 15 September 2000; accepted 6 December 2000

Abstract

A study is made of a polymer electrolyte system composed of poly(vinyl chloride) (PVC) as a host polymer, lithium tetrafluoroborate (LiBF_4) and lithium triflate (LiCF_3SO_3) as salts and a mixture of ethylene carbonate and propylene carbonate as plasticizers. X-ray diffraction (XRD) reveals that the salts and plasticizers disrupt the crystalline nature of PVC-based polymer electrolytes and converts them into an amorphous phase. Differential scanning calorimetry studies suggest that the plasticized samples have lower values of the glass transition temperature T_g , and thermogravimetric studies show that the thermal stability of the polymer electrolytes decreases with addition of plasticizers. The plasticized PVC electrolyte is used in the fabrication of electrochemical cells. The open-circuit voltage, discharge time for the plateau region, etc. are evaluated. © 2001 Elsevier Science B.V. All rights reserved.

Keywords: Polymer electrolyte; Plasticizer; PVC; Electrochemical cell

1. Introduction

In 1975, Wright [1] reported high ionic conductivity for mixtures of poly(ethylene oxide) (PEO) and alkali metal salts. Since then, polymer electrolytes have been of growing importance in applications which range from primary batteries to rechargeable batteries with high specific energy. Solid polymer electrolytes have many advantages, namely, high ionic conductivity, high specific energy, a solvent free condition, wide electrochemical stability windows, light and easy processability [2]. Apart from PEO, poly(vinyl alcohol) (PVA) [3], poly(vinyl chloride) (PVC) [4–6], poly(vinyl di fluoride) (PVDF) [7,8] and poly(acrylonitrile) (PAN) [9,10] have also been used as the polymer host material. In most solid polymer electrolytes, the polymer host is doped with inorganic salts and one or more plasticizers in order to enhance the conductivity. The conductivity is related to the glass transition temperature, T_g , and is further related to the inter-linking of the polymer chain, which makes the material more crystalline as confirmed by X-ray diffraction analysis (XRD) [11].

Many researchers have used XRD analysis to determine whether a material is amorphous or crystalline [12,13]. Solid-state chemistry has shown that polymers may form almost perfect crystals due to the spatial possibilities offered

by chain folding. The disruption of the crystalline peaks by certain types of modification, such as the addition of an inorganic salt and plasticizers, renders the final material more amorphous. Since only the amorphous phase contributes to the conductivity, amorphous materials will have better ionic conductivity than their crystalline counterparts [14].

It has also been suggested that an increase in T_g leads to a reduction in segmental motion of the polymer backbone, which finally results in a decrease in electrical conductivity [15]. In the present study, structural, thermal and electrochemical studies are performed on poly(vinyl chloride) (PVC)-based polymer electrolytes with LiBF_4 and LiCF_3SO_3 as salts and ethylene carbonate (EC) and propylene carbonate (PC) as plasticizers.

2. Experimental

2.1. Sample preparation

Films of PVC-based polymer electrolytes were prepared, using a single solvent, by means of the solution-cast technique. The PVC was obtained from Fluka, while lithium triflate (LiCF_3SO_3) and lithium tetrafluoroborate (LiBF_4) were obtained from Merck. The plasticizers, PC and EC, were both procured from Aldrich and Fluka, respectively.

* Corresponding author. Tel.: +60-3-759-4206; fax: +60-3-759-4146.

The solvent tetrahydrofuran (THF) was obtained from J.T. Baker.

Prior to the preparation of polymer electrolytes, LiCF_3SO_3 and LiBF_4 were dried at 100°C for 1 h in order to eliminate trace amounts of water. The required amounts of PVC and salts were dissolved separately in THF and these solutions were then mixed together and stirred. Different amounts of PC and EC were mixed and stirred for 24 h to achieve a homogeneous, viscous solution. The solution thus obtained was cast on a glass plate and allowed to evaporate slowly inside a dessicator.

2.2. Characterization techniques

2.2.1. Structural analysis

X-ray diffraction (XRD) analysis was performed with a Philips 1840 diffractometer using $\text{Cu K}\alpha$ radiation of wavelength $\lambda = 1.5418 \text{ \AA}$ for 2θ angles between 10° and 80° . The polymer films were scanned using a slit width of 0.05 and receiving slit of 0.2. The coherent length (\AA) was calculated from the Scherrer equation, i.e.

$$C = \frac{0.9\lambda}{\cos\theta_b(\Delta 2\theta_b)} \quad (1)$$

where λ is the X-ray wavelength; θ_b the glancing angle; $\Delta 2\theta_b$ the full width at half maximum (FWHM).

2.2.2. Thermal analysis

Differential scanning calorimetry (DSC) was performed with a Rheometric Scientific instrument and thermogravimetric analysis (TGA) with a Rheometric Scientific TGA 1000 instrument. The samples were heated at a rate of $10^\circ\text{C min}^{-1}$ at temperatures up to 300°C .

2.2.3. Electrochemical analysis

The polymer-salt-plasticizer film with the highest electrical conductivity was used as the electrolyte for secondary electrochemical cells. Graphite was chosen for the positive (cathode) electrode and lithium metal for the negative (anode). The cell was assembled in a casing, with the electrolyte sandwiched between the anode and the cathode materials, under an argon atmosphere in a glove box. Charge–discharge characteristics were obtained by means of a BAS LG50 galvanostat.

3. Results and discussion

3.1. Structural analysis (X-ray diffraction analysis)

X-ray diffraction measurements were conducted to examine the nature of the crystallinity of the polymer film with respect to pure PVC and to investigate the occurrence of complexation. The diffraction pattern for pure PVC is shown in Fig. 1(a). The sample is partially crystalline with peaks at 2θ angles of 13° and 16° . The patterns for

$[x\text{LiBF}_4 + (1-x)\text{LiCF}_3\text{SO}_3] + [\text{PVC}]$ complexes with $x = 0.2$ and 0.7 are presented in Fig. 1(b) and (c), respectively. Here, x is the weight fraction. The total weight of the salts is 1 g and the amount of PVC used in the preparation of the samples is also 1 g. The incorporation of lithium salts into the PVC matrix causes a shift in the PVC peaks to 2θ angles of 12.7° and 15.6° for $x = 0.2$, and to 12.9° and 15.7° for $x = 0.4$. This behaviour demonstrates that complexation has occurred between the salts and the polymer. The diffractograms show that there is a variation in the intensity of the PVC peaks. The amount of PVC and the total amount of salt is the same for all samples. The intensity of the peaks is expected to half when compared with the intensity of pure PVC. This is observed in Fig. 1(b). As more LiBF_4 is added, the intensity of the shifted PVC peaks is greatly reduced. This implies that the salts have also disrupted the crystalline region of the PVC and increased the amorphous region [11]. Complexation between the salts and the polymer takes place in the amorphous region [16]. This is conducted from the absence of the characteristic diffraction lines for the lithium salts in the diffractograms. Such changes in intensity and the shift of the peaks confirm complexation between PVC, LiCF_3SO_3 and LiBF_4 [17].

For the above system, XRD shows that the sample with $x = 0.7$ is the most amorphous sample. The amorphous/crystalline nature affects the electrical conductivity of the samples. The diffraction pattern for a PVC- LiCF_3SO_3 - LiBF_4 complex, which is plasticized with EC and PC is shown in Fig. 1(d). With the addition of EC and PC, the amorphous character of the sample is further increased and only one broad peak is observed. This broad peak is known as the ‘amorphous hump’ and is a typical characteristic of amorphous materials. The amorphous nature produces greater ionic diffusivity in accordance with the high ionic conductivity which can be obtained in amorphous polymers that have a fully flexible backbone [18].

From these diffractograms, the coherent or Scherrer length was calculated using the peak at $2\theta = 16^\circ$ and Eq. (1). The results are presented in Fig. 2. The sample with $x = 0.7$ has the smallest coherent length. Note, the length decreases with increase in the amorphous nature of the sample.

3.2. Differential scanning calorimetry (DSC)

The DSC thermogram of a pure poly(vinyl chloride) sample heated at a controlled rate is presented in Fig. 3(a). At the glass transition temperature, T_g , a small endothermic reaction is observed, i.e. the specific heat of the sample increases. The T_g for pure PVC is around 54°C . Beyond T_g , the plot remains virtually invariant until an exothermic reaction becomes evident when the sample releases heat during crystallization. This crystallization peak, T_c , is close to 162°C . Upon further heating, the initial stage of another endothermic peak is observed at around 280°C . This is the melting point of pure PVC [19,20].

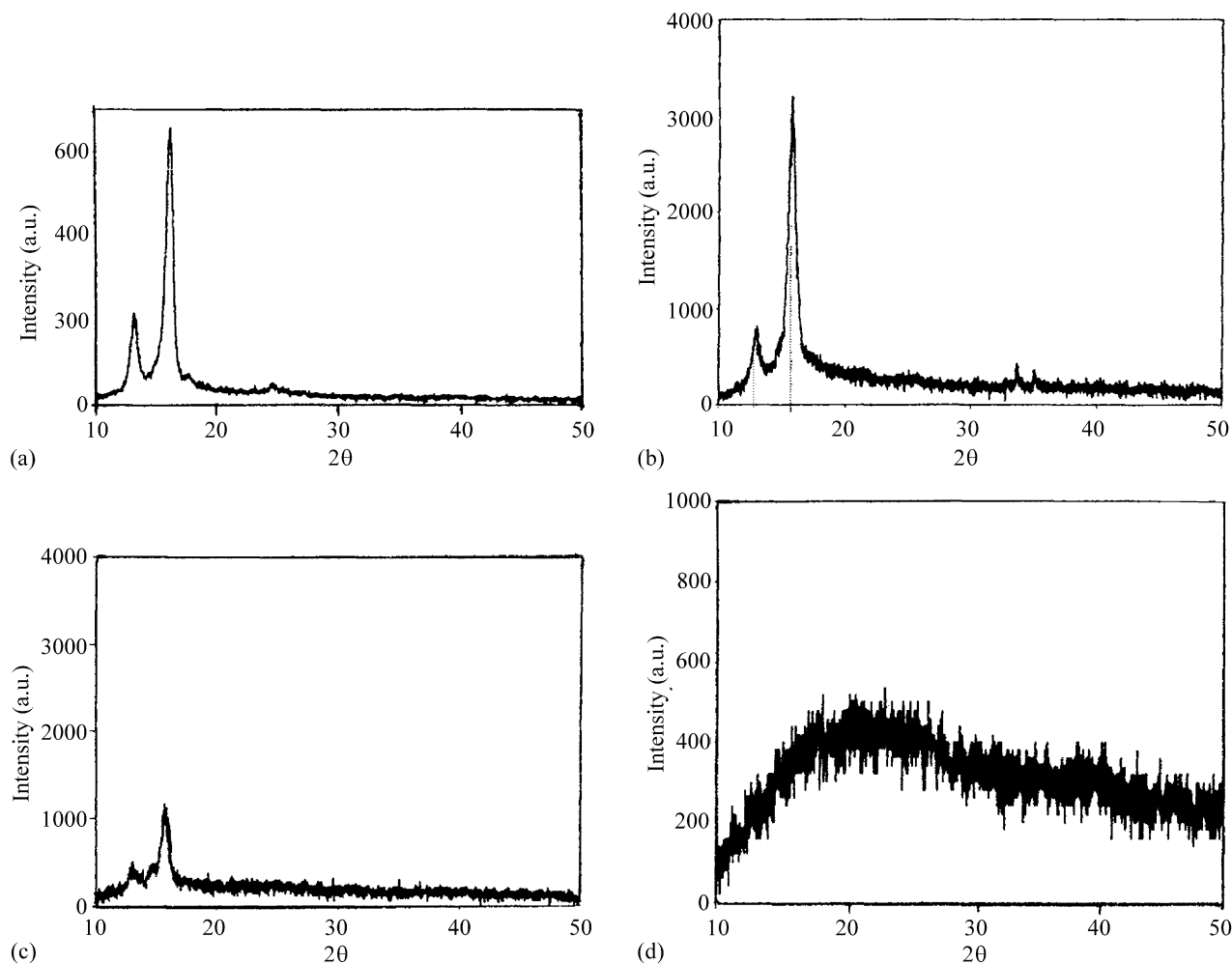


Fig. 1. Typical diffraction pattern for: (a) pure PVC; (b) $[x\text{LiBF}_4 + (1-x)\text{LiCF}_3\text{SO}_3] + [\text{PVC}]$ with $x = 0.2$; (c) $[x\text{LiBF}_4 + (1-x)\text{LiCF}_3\text{SO}_3] + [\text{PVC}]$ with $x = 0.7$; (d) PVC:LiBF₄:LiCF₃SO₃:EC:PC.

The DSC thermogram of $[x\text{LiBF}_4 + (1-x)\text{LiCF}_3\text{SO}_3] + [\text{PVC}]$ complex with $x = 0.7$ is given in Fig. 3(b). The value of T_g is around 73°C . This shows that the glass transition of the PVC-salt complex is shifted towards higher temperatures relative to PVC, which is expected on account of the lower

degree of chain movement caused by chlorine co-ordination. The cation-chlorine binding energy, which is the driving force for salt dissolution, contributes to the increase in the barrier to rotation of the polymer segments. This is indicated by a marked increase in the T_g for PVC-salt complexes

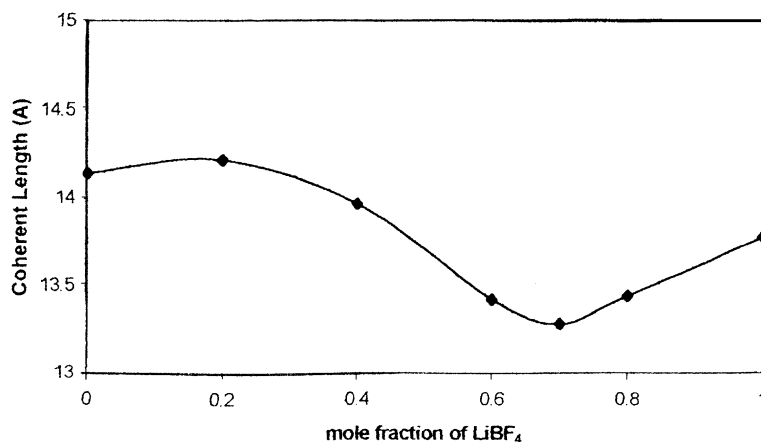


Fig. 2. Variation of coherent length as a function of mole fraction of LiBF₄ in $[x\text{LiBF}_4 + (1-x)\text{LiCF}_3\text{SO}_3] + [\text{PVC}]$ system.

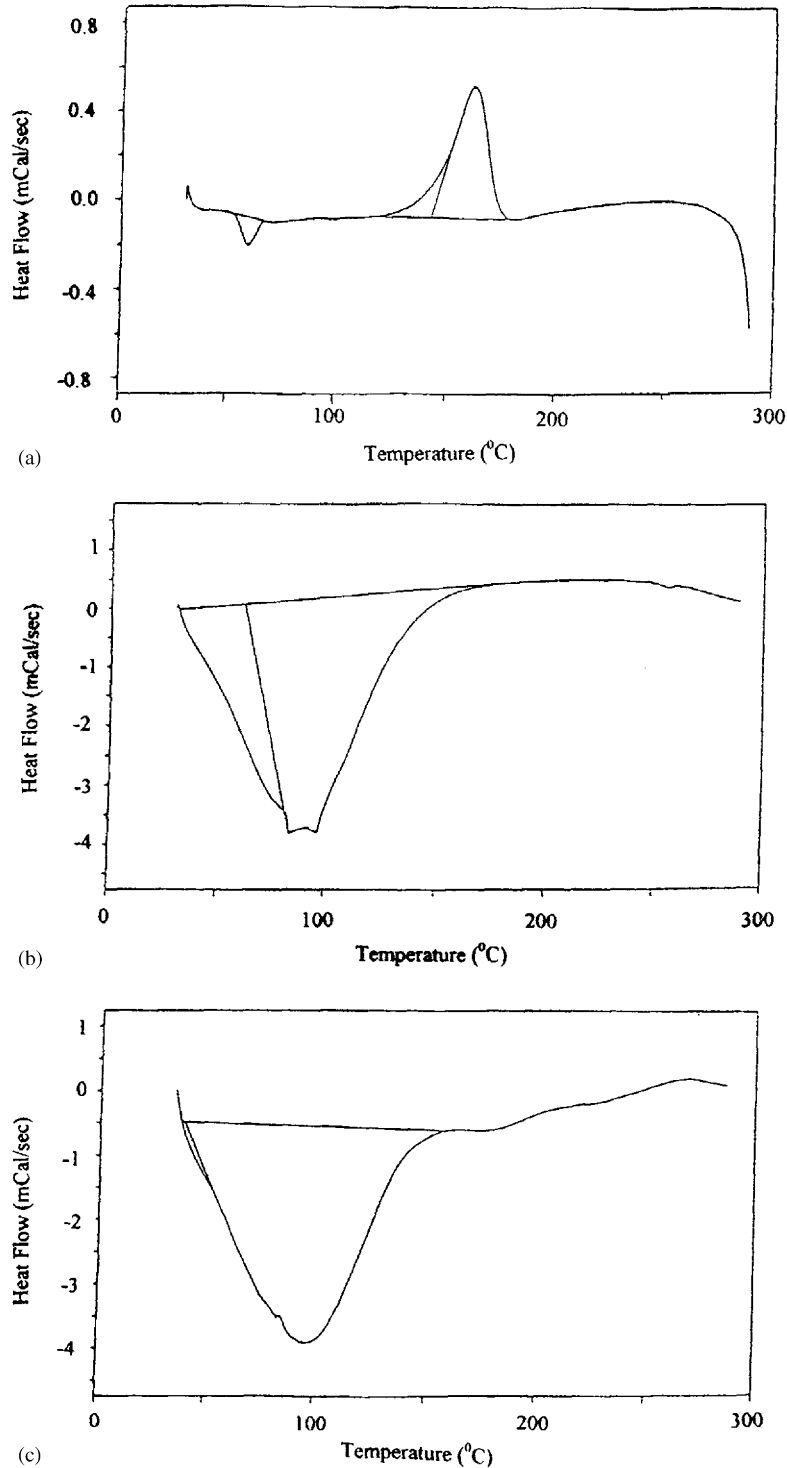


Fig. 3. DSC thermogram of: (a) pure PVC; (b) $[x\text{LiBF}_4 + (1-x)\text{LiCF}_3\text{SO}_3] + [\text{PVC}]$ with $x = 0.7$; (c) PVC:LiBF₄:LiCF₃SO₃:EC:PC.

[21,22]. Since the glass transition involves the freezing of large-scale molecular motions without a change in structure or the evolution of latent heat, it can be concluded that both LiCF₃SO₃ and LiBF₄ decrease local chain mobility. Accordingly, the crystallization peak and melting peak are shifted to higher temperatures and are therefore not shown in Fig. 3(b).

The DSC thermogram for the plasticized PVC-LiCF₃SO₃-LiBF₄ polymer electrolyte based on EC and PC is shown in Fig. 3(c). The T_g , which is calculated from Fig. 3(c), is 61°C. The plasticized sample presents a lower value of T_g than the plasticizer-free sample due to a lubricating effect [22]. Usually, the plasticizer behaves like a solvent when mixed with a polymer and results in a lowering of

the T_g value. This behaviour also confirms that the PVC has plasticized. The plasticization effect is related to a weakening of the dipole–dipole interactions due to the presence of the plasticizer molecules between the PVC chains [23]. The decrease in T_g helps to soften the polymer backbone and increase its segmental motion. Such segmental motion produces voids, which enables the easy flow

of ions through the material when there is an applied electric field.

3.3. Thermogravimetric analysis (TGA)

The thermogravimetric curve for pure PVC film is given Fig. 4(a). The film appears to be quite dry since its weight is

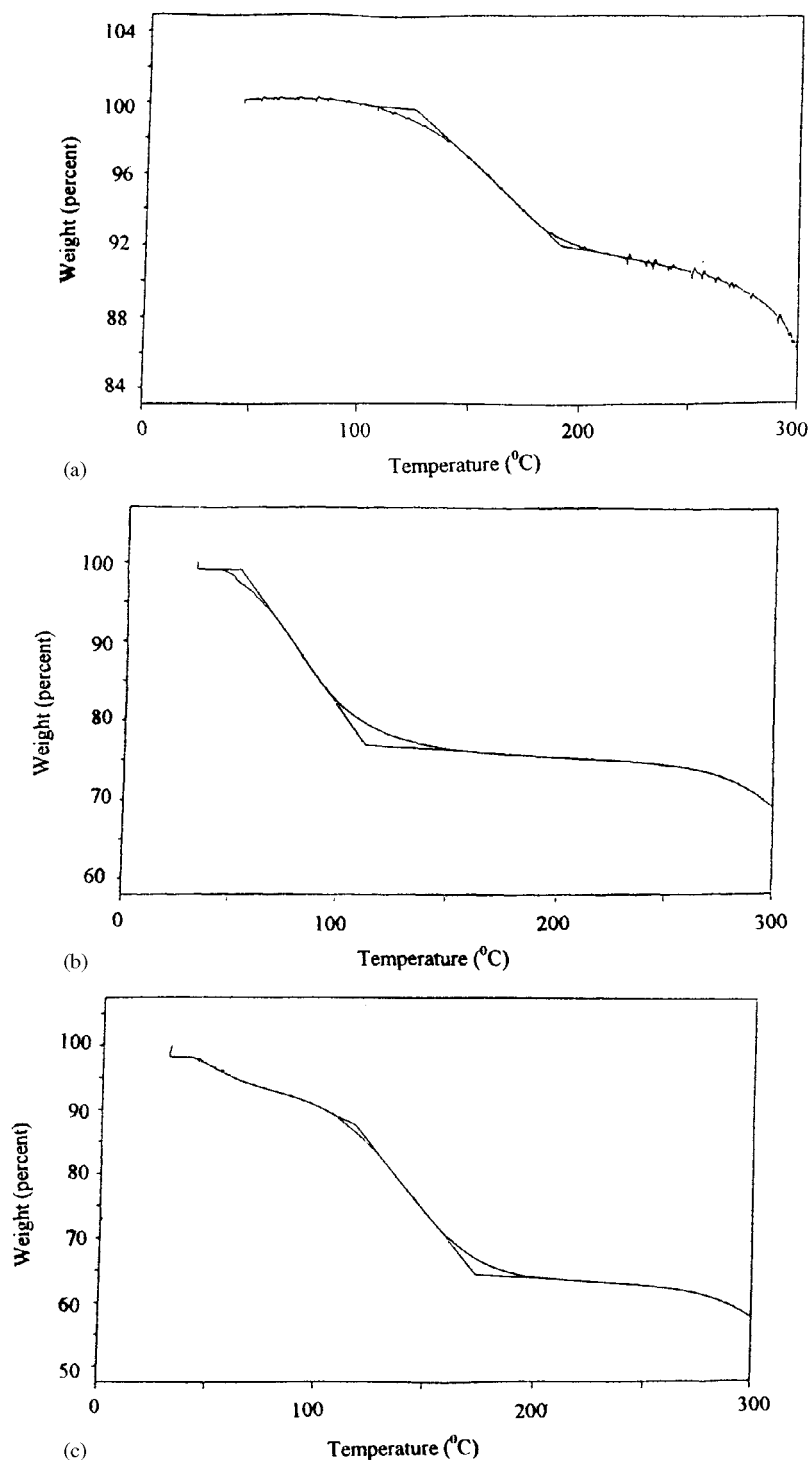


Fig. 4. Thermogravimetric analysis of: (a) pure PVC; (b) $[x\text{LiBF}_4 + (1-x)\text{LiCF}_3\text{SO}_3] + [\text{PVC}]$ with $x = 0.7$; (c) PVC:LiBF₄:LiCF₃SO₃:EC:PC.

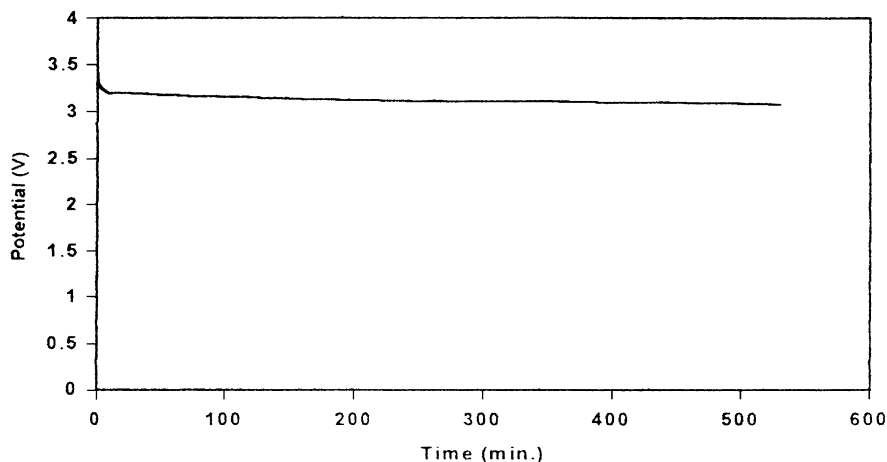


Fig. 5. Cell discharge characteristics for current drain of $I_d = 0.10$ mA.

almost constant up to 100°C . The significant weight loss which begins at temperatures above 100°C is due to crystallization of the sample, as confirmed by the DSC studies.

The TGA curve of the $[x\text{LiBF}_4 + (1-x)\text{LiCF}_3\text{SO}_3] + [\text{PVC}]$ complex with $x = 0.7$ is shown in Fig. 4(b). The sample starts to lose mass at temperature below 100°C . This initial loss results from residual solvent evaporation and the transition of the polymer electrolyte sample. Volatilization of monomers and oligomers adsorbed in the matrix can also be responsible for this initial mass loss [24]. The percentage weight loss for the mixed salt system is $\sim 24\%$. The second weight loss begins at a temperature of above 250°C . This may be due to the crystallization of the above polymer electrolyte samples. The increase in temperature of the second weight loss is a consequence of the increase in T_g value.

The TGA curve of double plasticizer complex. (PVC:LiCF₃SO₃:LiBF₄:EC:PC) is presented in Fig. 4(c). The data show that there is a weight loss of $\sim 7\%$ at a temperature below 100°C and $\sim 28\%$ at a temperature around 150°C . The second weight loss, as explained earlier,

is caused by crystallization of the polymer electrolyte. These results also indicate that the crystallization temperature is decreased compared with those for complexes. This may be due to a decrease in the T_g with respect to increase in plasticizer content. The thermal stability of the polymer electrolyte also decreases with the addition of plasticizer. This is because in the region between 100 and 150°C a weight loss of $\sim 28\%$ is observed compared with only $\sim 10\%$ for pure PVC.

3.4. Electrochemical analysis

The open-circuit voltage of the cell Li/PVC electrolyte/C was measured and found to be 3.4 V. The cell was discharged immediately. The discharge currents, I_d , applied were 0.10 and 0.50 mA. Typical discharge curves at these two currents are shown in Figs. 5 and 6, respectively.

The discharge curve for $I_d = 0.10$ mA has a voltage plateau at 3.1 V. This plateau is constant for at least 500 min. By contrast, for $I_d = 0.50$ mA, the curve displays two plateaus at 2.4 and 1.6 V. The cell voltage reaches zero

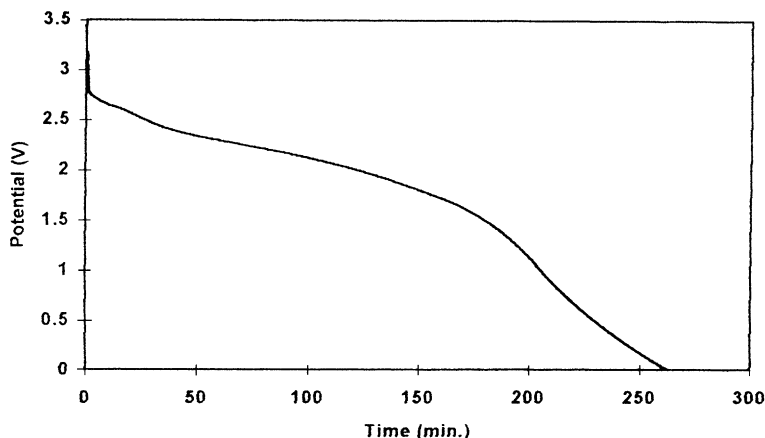


Fig. 6. Cell discharge characteristics for current drain of $I_d = 0.50$ mA.

after a prolonged time. The capacity of the cell fades away on extensive cycling. This may be attributed to several factors of which the most important is the formation of a non-conducting passivation film on the surface of the lithium electrode [25–28]. The lithium metal, which is used as an anode material in the present study, may interact with the chlorine atoms of the PVC polymer to form a surface layer of lithium chloride (LiCl). This is because the lithium metal has more affinity towards chlorine atoms of the PVC polymer. The formation of LiCl will automatically decompose the polymer electrolyte and thereby reduce the capacity of the thin-film polymer battery [29]. A further reason for the decreased capacity of the assembled cell may be the low ionic conductivity of the polymer electrolyte and high electrode/electrolyte interface resistance. This may be related to the deterioration of interfacial contact or contact loss at the electrode/electrolyte interface [28,30].

4. Conclusions

It is found that plasticized PVC electrolytes are in a more amorphous state compared with the unplasticized electrolytes. Evidence has also been obtained which shows that complexation has occurred between the salts and the polymer. The plasticized PVC polymer electrolytes have lower values of the glass transition temperature. The PVC-based polymer electrolyte films can be used as an electrolyte for a solid-state polymer cell although there is still room for improvement in the performance of this cell.

References

- [1] P.V. Wright, Br. Polymer J. 7 (1975) 319.
- [2] J.Y. Kim, S.H. Kim, Solid State Ionics 124 (1/2) (1999) 91–99.
- [3] P.K. Sukla, S.L. Agrawal, in: B.V.R. Chowdari, K. Lal, S.A. Agnihotry, N. Khare, S.S. Sekhon, P.C. Srivastava, S.Chandra (Eds.), Solid State Ionics: Science and Technology, World Scientific, Singapore, 1998, pp.211–216.
- [4] S. Ramesh, L. Rekha, S. Radhakrishna, A.K. Arof, in: B.V.R. Chowdari, K. Lal, S.A. Agnihotry, N. Khare, S.S. Sekhon, P.C. Srivastava, S. Chandra (Eds.), Solid State Ionics: Science and Technology, World Scientific, Singapore, 1998, pp. 201–205.
- [5] M. Alamgir, K.M. Abraham, J. Electrochem. Soc. 140 (1993) L96.
- [6] S. Ramesh, A.K. Arof, Solid State Ionics, submitted for publication.
- [7] J. Fuller, A.C. Breda, R.T. Carlein, J. Electrochem. Soc. 144 (1997) L67.
- [8] M.M.E. Jacob, A.K. Arof, Electrochim. Acta 45 (2000) 1701–1706.
- [9] H. Akashi, K. Tanaka, K. Sekai, J. Electrochem. Soc. 145 (1998) 881.
- [10] S.R. Starkey, R. Frech, Electrochim. Acta 42 (1997) 471.
- [11] N.S. Mohamed, M.Z. Zakaria, A.M.M. Ali, A.K. Arof, J. Power Sources 66 (1997) 169.
- [12] A.K. Arof, B. Kamaluddin, S. Radhakrishna, J. Phys. III (France) 3 (1993) 1201–1209.
- [13] J.L. Acosta, E. Morales, Solid State Ionics 85 (1996) 85–90.
- [14] J.R. Mac Callum, C.A. Vincent, Polymer Electrolytes Reviews 1 and 2, Elsevier, London, 1987 and 1989.
- [15] P.G. Bruce, Electrochim. Acta 40 (1995) 2077.
- [16] C. Carre, T. Hamaide, A. Guyot, C. Mai, Br. Polymer J. 20 (1988) 269–274.
- [17] P.N. Gupta, K.P. Singh, Solid State Ionics 86–88 (1996) 319–323.
- [18] R. Frech, S. Chintapalli, Solid State Ionics 85 (1996) 61–66.
- [19] J.V. Koleske, Poly(Vinyl Chloride), Macdonald Technical and Scientific Ltd., London, 1969.
- [20] S. Radhakrishna, A.K. Arof, Polymeric Materials, Narosa Publishing House, India, 1998.
- [21] A. Vallee, S. Besner, J. Prud'homme, Electrochim. Acta 37 (1992) 1579–1583.
- [22] E. Morales, J.L. Acosta, Solid State Ionics 96 (1997) 99–106.
- [23] V. Mano, M.I. Felisbersti, M.A. De Paoli, Macromolecules 30 (1997) 3026–3030.
- [24] V. Mano, M.I. Felisbersti, T. Matencio, M.A. De Paoli, Polymer 37 (1996) 5165–5170.
- [25] T. Nagatomo, C. Ichikawa, O. Omoto, J. Electrochem. Soc. 134 (1987) 305–308.
- [26] K.M. Abraham, M. Alamgir, Solid State Ionics 70/71 (1994) 20–26.
- [27] C.K. Huang, S. Surampudi, A.I. Attia, G. Halpert, in: Proceedings of the 182nd Electrochemical Society, Toronto, Canada, 1992.
- [28] F. Bonino, M. Ottaviani, B. Scrosati, J. Electrochem. Soc. 135 (1998) 12–15.
- [29] J.M. Tarascon, C. Schmutz, A.S. Gozdz, P.C. Warren, F.K. Shokoohi, Presented at the Materials Research Society Meeting, Boston, MA, 1994.
- [30] D.W. Kim, Y.K. Sun, J. Electrochem. Soc. 145 (1998) 1958–1963.